ANTIMICROBIAL AGENTS AND CHEMOTHERAPY, May 2005, p. 1890–1897 Vol. 49, No. 5
0066-4804/05/$08.00+0 doi:10.1128/AAC.49.5.1890–1897.2005

Mechanism of Action of a Novel Series of Naphthyridine-Type Ribosome Inhibitors: Enhancement of tRNA Footprinting at the Decoding Site of 16S rRNA

Linus L. Shen,* Candace Black-Schaefer, Yingna Cai, Peter J. Dandliker, and Bruce A. Beutel

Infectious Diseases Research, Abbott Laboratories, Abbott Park, Illinois 60064

Received 21 July 2004/Returned for modification 1 October 2004/Accepted 4 January 2005

The novel ribosome inhibitors (NRIs) are a broad-spectrum naphthyridine class that selectively inhibits bacterial protein synthesis (P. J. Dandliker et al., Antimicrob. Agents Chemother. 47:3831–3839, 2003). Footprinting experiments, using a range of NRIs and chemical modification agents on *Escherichia coli* ribosomes, revealed no evidence for direct protection of rRNA. In the presence of tRNA, however, we found that NRIs enhanced the known ribosomal footprinting pattern of tRNA in a dose-dependent manner. The most prominent increase in protection, at A1492/3 and A1413 in helix-44 of 16S RNA, strictly required the presence of tRNA and poly(U), and the effect was correlated with the potency of the inhibitor. Radioligand binding studies with inhibitor [^{3}H]A-424902 showed that the compound binds to tRNA, either in its charged or uncharged form. The dissociation constant for [^{3}H]A-424902 binding to Phe-tRNA^{Phe} was determined to be 1.8 μM, near its translation inhibition potency of 1.6 μM in a cell-free *S. pneumoniae* extract assay. The compound did not change the binding of radiolabeled tRNA to the 30S ribosomal subunit. Taken together, these results imply that the NRIs exert their effects on protein synthesis by structurally perturbing the tRNA/30S complex at the decoding site.

Ribosomes are macromolecular protein-biosynthetic machinery against which many effective antibacterial agents act. The ribosome is a proven antibacterial target (10, 37). Inhibitors that bind the large (50S) ribosomal subunit include macrolides, lincosamides, streptogramins, chloramphenicol, oxazolidinones. These antibiotics usually target the central loop in domain V of 23S rRNA, affecting one or more steps in transpeptidation, translocation, peptide bond formation, or peptide elongation. The 30S inhibitors mainly include aminoglycosides and tetracyclines that inhibit or alter the translation step in protein synthesis by interfering with the decoding process. The high-resolution X-ray crystal structures of ribosomal subunits and their complexes with many ribosome inhibitors have been determined recently, providing remarkable insights into the details of drug-rRNA interactions (2, 3, 18, 25, 33–35). Recently, we discovered a class of novel ribosome inhibitors (NRIs) that exhibit broad-spectrum antibacterial activity and the ability to inhibit the growth of important pathogens such as *Streptococcus pneumoniae*, *Haemophilus influenzae*, *Staphylococcus aureus*, and *Moraxella catarrhalis* that are known to be important in respiratory infections (4, 5). Analysis of NRI-resistant mutants (5) indicated that a single mutation in the ribosome is sufficient to confer resistance. This observation is consistent with the notion that the NRIs act by binding to the ribosome, but a precise binding site of these inhibitors has not yet been identified. Because NRI-resistant strains are not resistant to known ribosome inhibitors such as macrolides, chloramphenicol, tetracycline, aminoglycosides, or oxazolidinones, we believe the NRI series interacts with the ribosome in a unique way, possibly at a unique site. In order to better understand the NRI mechanism of action and potentially identify a ribosome binding site, we undertook chemical footprinting studies, monitored by primer extension, a powerful tool in mapping the drug interaction sites on ribosomes (11, 13, 14, 17, 19, 22). In the present study, we show that the NRIs affect the tRNA interaction with 16S rRNA at the decoding region that includes A1492/3 and A1408, A1413 in helix 44. These results imply that the NRIs affect the tRNA interaction with the small ribosomal subunit at the decoding site.

* Corresponding author. Mailing address: Abbott Laboratories, Department R47R, Bldg. AP10, 100 Abbott Park Rd., Abbott Park, IL 60064-6099. Phone: (847) 937-5983. Fax: (847) 938-1674. E-mail: linus.l.shen@abbott.com.

MATERIALS AND METHODS

Materials. All uncharged tRNAs, dimethyl sulfate, and antibiotics were purchased from Sigma Chemical Co. (St. Louis, MO), except for linezolid, fusidic acid, and [^{3}H]A-424902 (specific activity, 9.78 Ci/mmol), which were synthesized at Abbott. Preparations of tRNA^{Phe} and the charged Phe-tRNA were also obtained from Francisco Javier Triana-Alonso, (Centro de Investigaciones Biomedicas, Universidad de Carabobo Nucleo Aragua, Aragua, Venezuela). Avian myeloblastosis virus reverse transcriptase was from Roche Molecular Biochemicals (Indianapolis, IN). ddNTP and dNTP were purchased from Invitrogen, Inc. [γ-^{33}P]ATP was obtained from Perkin-Elmer Life Sciences, Inc. (Boston, MA). The 70S ribosome was isolated from *Escherichia coli* MRE600 cells using published procedures (1), except that a bead-beater method (26) with 0.1-mm silica beads (Biospec Products, Inc., Bartlesville, OK) was used for breaking the bacterial cells. The ribosomal 30S subunit was purified from crude 70S ribosomes by sucrose-gradient centrifugation (32). The 30S ribosomal subunit was activated by heating in modification buffer at 42°C for 20 min immediately before the experiment.

DMS footprinting. Methods of chemically probing the tRNA binding site on 16S rRNA were based on the procedures described by Noller and coworkers (17, 31) with minor modifications. The sequence of the oligonucleotide primer used for probing theA1408 to A1494 region in 16S rRNA was: GAGGTGATCCAA CCGCAGGTTCC (nucleotide [nt] 1516 to 1538). The primer was end labeled with [γ-^{33}P]ATP by using polynucleotide T4 kinase (Invitrogen, Calsbad, CA), and the labeled product was purified by gel-filtration by using a Micro-Select-D

G-25 kit (VWR Scientific Products, Bristol, CT). Chemical modification of ribosome subunits with dimethyl sulfate (DMS) was carried out in microcentrifuge tubes with 50-μl reaction mixture containing 50 pmol of ribosomal subunit and various concentrations of test compound in modification buffer (80 mM sodium cocadylate [pH 7.2], 25 mM $MgCl_2$, 100 mM ammonium chloride). After 20 min incubation at 37°C, the mixture was treated with 2 μl of DMS (12.5% in ethanol) with 10 min of incubation at 37°C. The modification reaction was terminated by adding 25 μl of stop solution (1 M Tris-acetate [pH 7]; 1.5 M sodium acetate, 1 M β-mercaptoethanol and 0.1 M EDTA). The mixture was cooled on ice for 10 min, and the oligonucleotides were precipitated by adding 180 μl of cold 95% ethanol. The precipitates were kept at −20°C for at least 30 min before being collected by 15 min of centrifugation at 4°C, and the samples were resuspended in 100 μl of Tris-EDTA buffer. rRNA was isolated by using RNeasy Minikits (Qiagen, Inc., Valencia, CA), and the nucleotide concentration was determined spectrophotometrically. The samples were diluted with water to a final nucleotide concentration of 1 μg/μl prior to the primer extension reaction.

Primer extension. The rRNA modification sites were analyzed by primer extension analysis with avian myeloblastosis virus reverse transcriptase (Roche Molecular Biochemicals, Indianapolis, IN). Hybridization reactions were carried out in 96-well PCR plates containing rRNA (3 μg) and 3 pmol ^{33}P-end-labeled primer in a final volume of 8 μl in hybridization buffer (50 mM HEPES [pH 7.2] and 100 mM KCl) by using a PCR thermocycler (Perkin-Elmer model 9600 GeneAmp PCR System), with an initial incubation at 94°C for 2 min and then a linear ramp of the temperature to 42°C in 30 min, followed by incubation at 42°C until used. Primer extension was carried out in the same plate by adding 8 μl of a prewarmed solution of reverse transcriptase (8 U per well) and deoxynucleoside triphosphate (250 μM each) in a buffer containing 130 mM Tris-HCl (pH 8.5), 10 mM $MgCl_2$, and 10 mM dithiothreitol, followed by incubation for 30 min at 40°C. At the end of the incubation, 210 μl of stop solution (0.3 M sodium acetate [pH 5.5] in 74% ethanol) was added, and the mixture (enough for two repeats of the subsequent experiments) was separated into two sets of microcentrifuge tubes and stored at −80°C. Multichannel pipettes were used for all of the liquid handling to increase throughput and to assure uniform reaction times. For electrophoretic determination of the cDNA primer extension products, one set of the mixtures was removed from the freezer and centrifuged for at least 45 min at maximum speed. The supernatants were aspirated, and the precipitates were dried for 5 min in a bench-top vacuum microcentrifuge. The dried products were dissolved in 10 μl of loading buffer (80% deionized formamide, 10 mM EDTA, 1 mg of xylene cyanol/ml, and 1 mg of bromophenol blue/ml). The samples (1 μl per lane) were loaded onto Bio-Rad 6% polyacrylamide sequencing gels and electrophoresed for ca. 2 h until the blue tracking dye reached the bottom end of the gel. The gel, after being blotted and dried on filter paper, was scanned on a PhosphorImager (Storm 860; Molecular Dynamics, Amersham Biosciences, Piscataway, NJ), and the cDNA bands were analyzed by using ImageQuant software. The band intensity at sites of our interests was quantitatively determined by using a densitometric analysis software (Scion Image for Windows; Scion Corp., Frederick, Maryland).

***S. pneumoniae* translation inhibition assay.** The detailed procedures for the luciferase-readout translation assay using *S. pneumoniae* S30 extract have been described previously (5, 20).

Binding assays. The binding of radiolabeled NRIs to tRNA was performed by equilibrium dialysis using Dispo Dialyzer devices (Harvard Biosciences) that have a volume capacity of 50 μl on each side of a 10-kDa cutoff membrane. An aliquot (50 μl) of binding mixture consisting of 0.1 μM radiolabeled [^{3}H]A-424902 in binding buffer (20 mM HEPES [pH 7.6], 4.5 mM magnesium acetate, 150 mM potassium acetate, 2 mM spermidine, 4 mM β-mercaptoethanol) was placed on one side of the membrane. On the opposite side of the membrane, it was placed with 10 μM Phe-tRNA in the same volume of binding buffer. The dialysis was carried out for 24 h at 4°C. For binding experiments at higher ligand concentrations, unlabeled A-424902 was added to raise the total ligand concentrations up to 150 μM. Then, 25-μl aliquots were removed from each side of the membrane, and the amount of bound ligand was determined as the difference in radioactivity between the two sides. Free ligand concentrations were determined from the radioactivity at the ligand side. All datum points were generated in duplicate. The binding data were presented in a Klotz Plot (8) in which the molar binding ratio was plotted against the free ligand concentration (27, 30). The resulting binding isotherm can be fitted with the Hill equation by using SigmaPlot software (SPSS, Inc., Chicago, IL).

The binding of radiolabeled tRNA with 30S ribosomal subunits was measured by using nitrocellulose filters as previously described (9). Deacylated $tRNA^{Phe}$ was labeled by using T4 polynucleotide kinase and [γ-^{33}P]ATP. Binding mixtures (in a final volume of 50 μl) consisted of 1 μM activated 30S subunit, 30 nM radiolabeled tRNA, cold tRNA (when higher total tRNA concentrations were needed), 20 μg of poly(U), and various concentrations of A-424902 (from 10 to 100 μM) in modification buffer. After 20 min of incubation at 37°C, the mixtures were diluted to 1 ml with modification buffer, filtered through a nitrocellulose filter (Millipore Co.), and washed twice with the 2 ml of the same buffer. Filters were dried for 30 min under a heat lamp, and the retained radioactivity was determined by scintillation counting.

RESULTS AND DISCUSSION

NRIs alter the tRNA footprint on 16S rRNA. We carried out extensive chemical footprinting efforts on the entire *E. coli* 70S ribosome in an attempt to map the NRI interaction sites. Such efforts turned out to be fruitless since no footprinting site was found on either subunit. Our preliminary finding that the drug bound to tRNA (see later section and Fig. 5) prompted us to examine the tRNA footprinting pattern on ribosomal subunits in the presence of the inhibitor. We probed the known tRNA protection sites against chemical footprinting on the entire 50S (15) and 30S (16) ribosomal subunits. It was seen that the NRI compounds promoted a tRNA protection effect and resulted in weaker footprinting bands, and this increase in protection was particularly evident at sites on 16S rRNA. These included sites at A532, A790, A792, A794/5, A1408, A1411, and A1492/3 in 16S rRNA. To further investigate the drug effects, we focused on probing the most prominent 16S sites at A1408, A1411, and A1492/3 that consist of the A-site decoding region (Fig. 1), which has been shown to be the major target sites of many antibiotics (6, 7, 12, 14, 21, 23, 33–36). The drug effect on the increased tRNA protection at these adenosine sites can be studied conveniently by DMS probing alone. DMS methylates adenine at N-1, guanine at N-7, and cytosine at N-3, but only the adenine and cytosine methylatons inhibit the progress of reverse transcriptase (31). Since the extent of the chemical modification was very limited, only those highly reactive adenine and cytosine were modified resulting in visible gel bands that are radiolabeled cDNA molecules terminated at this particular modified nucleotide. The intensity of the band is proportional to the reactivity of the base. When the band intensity decreases in the presence of a binding ligand, it can normally be interpreted as the ligand-interaction sites due to protection through direct binding or indirect allosteric effects. Also shown in these gel autoradiograms (Fig. 2 to 4) are intense bands across all of the lanes; these are strong termination stops due to secondary structures of the RNA template (31). Figure 2A shows the autoradiograph demonstrating the effect of A-424902, one of the most active NRI analogs (see structure and potency values in Table 1), on these tRNA protection sites. The results of densitometric analysis of band intensity at the sites of our interests are shown in Fig. 2B (for the A1413 site) and Fig. 2C (for the A1492/3 sites). The increased tRNA protection effect, i.e., a sharper decrease in band intensities as a function of tRNA concentration in the presence of the drug is obvious, and the effect is more distinct with a subeffective level of poly(U) (0.4 μg/μl) at which the tRNA effect in the absence of the drug has not reached the maximum. At a higher poly(U) concentration (0.8 μg/μl), the stronger tRNA protection effect evidently masks the drug effect. The dependence on tRNA concentration can be clearly seen in the presence of the drug: with a marginal effect at 1 μM and a strong effect at >2 μM tRNA. It was interesting to see that the decrease in band intensity at A1492/3 paralleled that at A1413, located 5 nt away

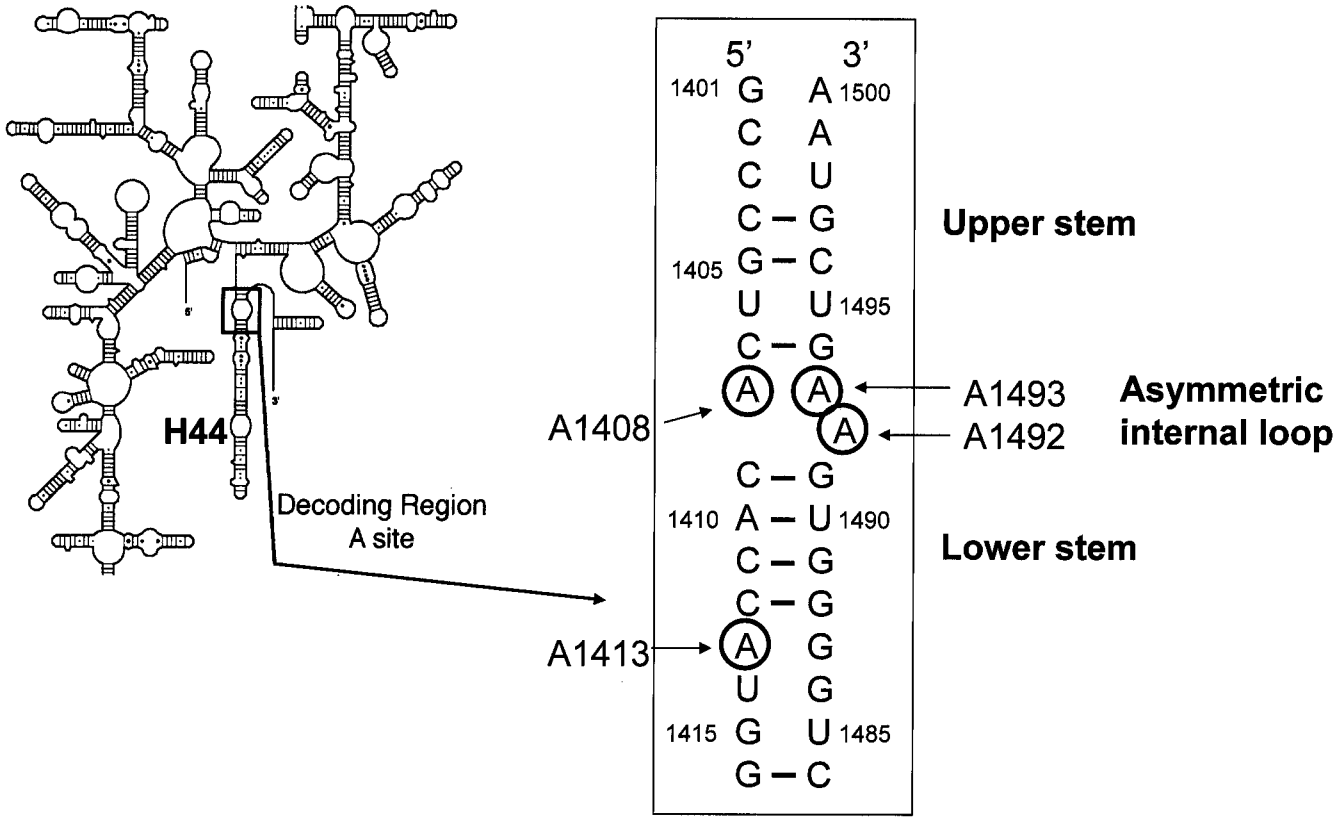

FIG. 1. Secondary structure of the A-site decoding region in 16S rRNA. The information shown here was obtained from references 7, 21, and 24.

from the asymmetric internal loop below the lower stem (Fig. 1). It should be noted that such parallelism can only be observed from results with the use of tRNA (Table 2).

Figure 3 shows the increased tRNA protection induced by other NRI compounds (see structure and translation inhibition potency in Table 1). The data for tetracycline and streptomycin are also included for comparison. The effect at A1492/3 and A1413 is dose dependent and shows clearly an increased protection at 10 μM for the more potent compounds A-424902, A-358816, and A-362505, whereas A-548501, an inactive compound (Table 1), shows no protection effect. The only exception is A-438301, which is active in our bacterial translation assay (IC_{50} = 9.2 μM) but shows no effect on tRNA footprinting. Notably, A-438301 also behaves differently from the other NRIs in that it does not compete with radiolabeled A-424902 for binding to the Phe-$tRNA^{Phe}$ (Table 1), indicating a different binding or inhibition mode. Consistent with the conclusion that the increased protection effect requires poly(U), no effect was observed when poly(U) was replaced by poly(A). Also shown in Fig. 3, tetracycline, a 30S subunit inhibitor that was shown to bind to helix-34 did not show such increased protection effect up to 100 μM, whereas streptomycin, a helix-44 binder, showed a strong effect at 10 μM. The observation that the increased protection effect correlated with the inhibitory potency of the compounds renders an important piece of evidence that NRIs capability to alter the tRNA interaction with 16S rRNA at the decoding site may be relevant to its mode of action.

A comparison of the increased protection effects of NRIs with paromomycin and streptomycin at lower concentrations is shown in Fig. 4. In the presence of tRNA and poly(U) (see the left half of Fig. 4), we saw increased protection at A1492/3 with 1 μM paromomycin and streptomycin, with 4 μM A-358816, and with 10 μM A-362505. We also probed the same region of rRNA to look for direct effects of the test compounds in the absence of tRNA/poly(U). Figure 4 (right portion) illustrates that the NRIs did not show such direct effects at any of these sites. In contrast, streptomycin (1 μM) and paromomycin (4 μM) showed a distinct direct protection effect at A1413. Paromomycin (4 μM) also affected A1408 in the absence of tRNA. In the absence of tRNA, none of the compounds had any effect at A1492/3.

In order to learn whether the pattern of increased protection induced by compounds in the NRI series was common to any other ribosomal inhibitors, we performed the same set of experiments with a range of antibacterials. The results are summarized in Table 2. Of these inhibitors, none of the 50S binders, as expected, induced any change in the protection pattern in the 30S decoding region either in the presence or absence of tRNA. Among the 30S subunit inhibitors, results obtained in the presence of tRNA and poly(U) can be divided into three groups: (i) apramycin, gentamicin, kanamycin, neomycin, and

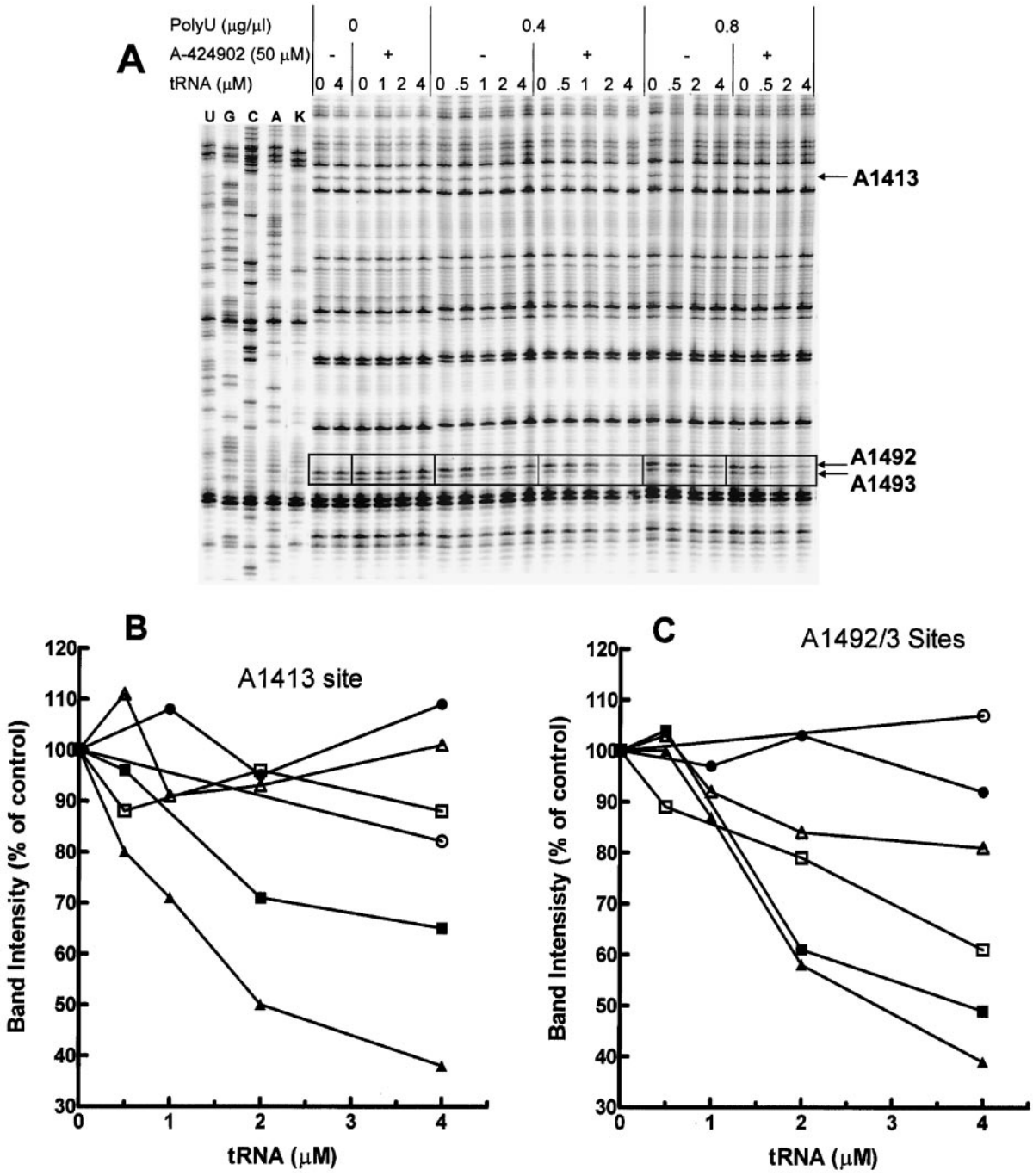

FIG. 2. (A) Autoradiograph showing A-424902 induced alterations in the DMS reactivity of A1492/3 and A1413 in helix-44 of 16S rRNA in the presence of various amounts of tRNA and poly(U). *E. coli* 30S ribosomal subunits (50 pmol) were incubated with 50 μM drug for 20 min in a volume of 50 μl prior to DMS treatment as described in Materials and Methods. U, G, C, and A denote dideoxynucleotide sequencing lanes; K denotes unmodified rRNA. Positions with altered reactivity are indicated by arrows. Reverse transcriptase stops 1 nt ahead of the corresponding nucleotide in the sequencing lanes; therefore, a band in the modified RNA footprinting gel corresponds to the band one position up in the sequencing lanes. (B and C) Band intensities at the A1413 site and the A1492/3 sites were determined by densitometric analysis. The band intensity, expressed as the percentage of the intensity relative to that without tRNA, is plotted against tRNA concentrations. The results were obtained with (filled symbols) or without (open symbols) the compound A-424902, with poly(U) concentrations at 0 μg/μl (circles), 0.4 μg/μl (triangles), and 0.8 μg/μl (squares).

paromomycin, which increase tRNA protection at all three sites (A1408, A1413, and A1492/3); (ii) streptomycin and hygromycin B, which do not affect tRNA protection at A1408 but increase protection at both A1413 and A1492/3; and (iii) kasugamycin, spectinomycin, tetracycline, and puromycin, none of which bind to helix-44, which show no effect at any of these sites. In the absence of tRNA and poly(U), inhibitors from groups i and ii have variable effects on the A-1413 and A1408

TABLE 1. Chemical structure and activities of naphthyridine-type ribosome inhibitors

Compound	Structure	*S. pneumoniae* in vitro translation (IC_{50} [μM])	Effect of A1492/3 footprinting sites[a]	Competition with [^{3}H]A-424902 for binding to Phe-tRNA^{Phe}[b]
A-72310	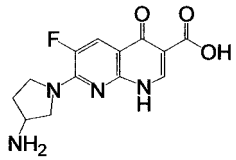	5	++	+
A-692345	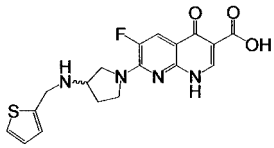	14	+	NT
A-424902	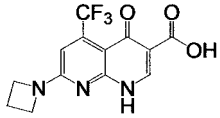	1.6	+++	+
A-358816	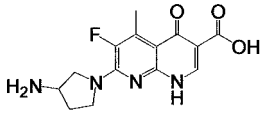	1	+++	+
A-362505	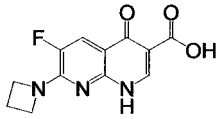	5	+++	+
A-438301	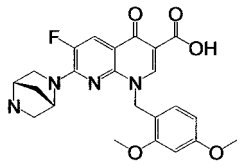	9.2	−	−
A-548501	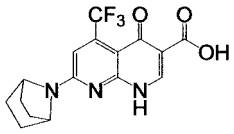	>200	−	NT

[a] "+++", "++", and "+" denote strong (IC_{50} < 20 μM), moderate (IC_{50} = 21 to 100 μM), and weak (IC_{50} > 100 μM) effects, respectively, on the increase in tRNA protection.
[b] "+" and "−" denote positive and negative competition effects, respectively. NT, not tested.

sites, but none of them has any effect at the A1492/3 sites. The group iii inhibitors again have no effect at any of these sites. Upon examining the patterns of increased protection by these drugs in Table 2, we found that the NRIs share behavior with some of these other inhibitors but that the NRI patterns are distinct, a finding consistent with a different mode of interaction. These data suggest that the NRIs most likely interact with the 30S ribosomal subunit but do so in a way that is not identical to the other ribosome inhibitors shown in Table 2. We caution that while these data may suggest that the NRIs interact with helix 44, they are insufficient to definitively make this conclusion. In order to identify the NRI binding site, additional studies will be required.

Radioligand binding studies. The radioligand binding method is a powerful tool in investigating small ligand interactions with macromolecules, exemplified by the quinolone antibacterial binding to DNA and DNA gyrase (27–30). We synthesized here [^{3}H]A-424902 to investigate NRI binding to

TABLE 2. Effect of ribosome-targeted antibiotics and NRIs on tRNA protection at the decoding site in 16S rRNA

Inhibitor	Protection[a]:						Binding domain in 30S
	With tRNA and poly(U)			Without tRNA and poly(U)			
	A1492/A1493 sites	A1413	A1408	A1492/A1493 sites	A1413	A1408	
30S inhibitors							
Apramycin	+	+	+	−	+	−	NA
Gentamicin	+	+	+	−	+	+	H44
Kanamycin	+	+	+	−	−	−	H44
Neomycin	+	+	+	−	+	+	H44
Paromomycin	+	+	+	−	+	+	H44
Streptomycin	+	+	−	−	+	−	H44
Hygromycin B	+/−	+/−	−	−	−	−	H44
Kasugamycin	−	−	−	−	−	−	H24
Spectinomycin	−	−	−	−	−	−	H34
Tetracycline	−	−	−	−	−	−	H34
Puromycin	−	−	−	−	−	−	NA
50S inhibitors							
Linezolid	−	−	−	−	−	−	
Chloramphenicol	−	−	−	−	−	−	
Fusidic acid	−	−	−	−	−	−	
Kirromycin	−	−	−	−	−	−	
Sparsomycin	−	−	−	−	−	−	
NRIs							
A-72310	+	+	−	−	−	−	
A-692345	+	+	−	−	−	−	
A-424902	+	+	−	−	−	−	
A-358816	+	+	−	−	−	−	
A-362505	+	+	−	−	−	−	
A-438301	−	−	−	−	−	−	
A-548501	−	−	−	−	−	−	

[a] "+" denotes increased tRNA protection on the specified 16S rRNA sites with >70% band intensity reduction at 100 μM drug compared to that observed in the absence of the drug; "+/−" denotes a weak effect with 30 to 70% band intensity reduction at 100 μM; "−" denotes a lack of protection effect with <30% band intensity reduction at 100 μM. NA, not available or known.

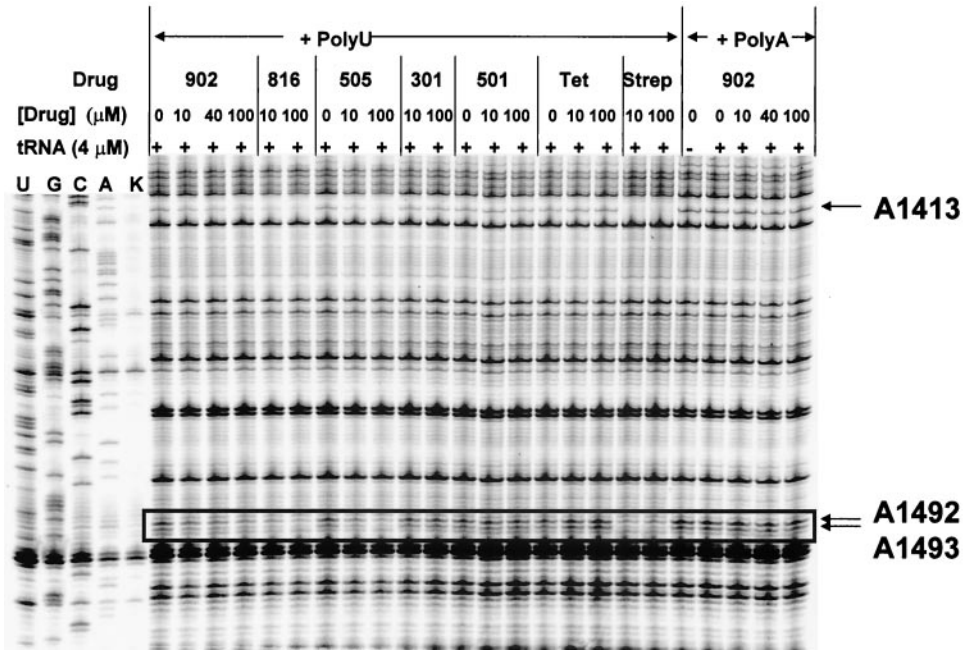

FIG. 3. Effect of NRIs, tetracycline (Tet), and streptomycin (Strep) on DMS modification of bases in the decoding region of 16S rRNA and its dependence on tRNA and poly(U). "+" or "–" denote the presence or absence of $tRNA^{phe}$ (6 μM) in the reaction mixture, respectively. The poly(A) and poly(U) concentrations were 0.4 μg/μl.

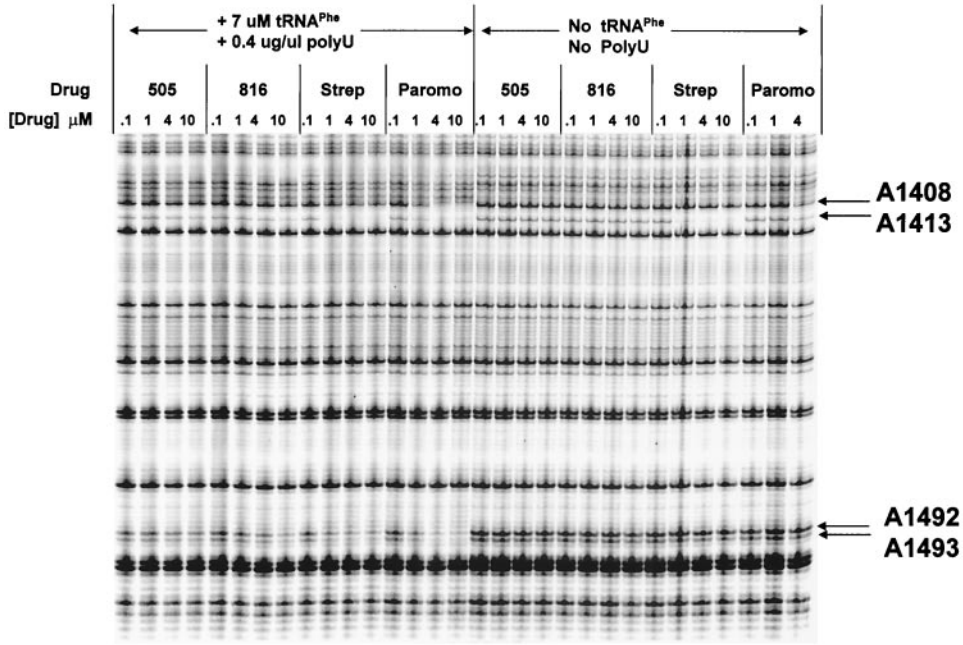

FIG. 4. Comparison of the effect of NRI, streptomycin, and paromomycin at low concentrations on DMS modification in the presence or absence of tRNA. The concentrations of $tRNA^{phe}$ and poly(U), when present, were 7 μM and 0.4 μg/μl, respectively. Paromo, paromomycin; Strep, streptomycin; 505, A-362505; 816, A-358816. Other abbreviations are as defined in the legend to Fig. 2.

components in the bacterial translation machinery. We observed binding of this labeled compound to both ribosomal subunits, but whether such bindings were specific or nonspecific remains to be established (L. L. Shen, unpublished results). In the course of our studies, we also made the unexpected observation that [^{3}H]A-424902 interacted with tRNA in both its charged and uncharged forms and bound preferentially to $tRNA^{Phe}$ (data not shown). We thus used Phe-$tRNA^{Phe}$ as our model receptor to study the drug binding in detail. Figure 5 shows the binding of [^{3}H]A-424902 to Phe-tRNA in the drug concentration range from 0.1 to 150 μM. The binding isotherm is presented as a Klotz Plot (8) of molar binding ratio versus free drug concentration. The isotherm can be fitted by using the Hill equation with noncooperative binding (Hill constant = 1) and a dissociation constant equal to 1.8 μM. The molar binding ratio reaches a plateau at ca. 1 NRI/tRNA at high drug concentrations (there is no further large increase in the molar binding ratio at between 10 and 100 μM A-424902). In these experiments, the labeled drug concentration was kept constant as the unlabeled A-424902 concentration was varied. The increased scatter in datum points at the higher ligand concentrations was due to the low counts per minute bound (resulting from high dilution of radiolabeled A-424902 by cold A-424902). It is intriguing that the K_d value (1.8 μM) measured here for A-424902 is similar to the translation inhibition IC_{50} value (1.6 μM) for the inhibitor (Table 1). This provided another piece of evidence indicating that the drug binding to tRNA may be relevant to the inhibitory mechanism. Quinolone antibacterials have been shown to bind to nucleic acids, especially to single-stranded forms, as their mechanism of action (27, 30); it is therefore not surprising to see that the NRIs bind to tRNA, a nucleic acid species rich in single-stranded regions. Whether magnesium ions play a role in drug binding through a chelating effect remains unclear. Since footprinting and translation assay require the divalent ion for the validity of the experiments, a test of the magnesium effect experimentally is less likely. Besides, it is unclear whether the binding to tRNA is directly or indirectly responsible for the inhibition of ribosome function. Also, it needs to be confirmed that the existence of a single drug binding site on

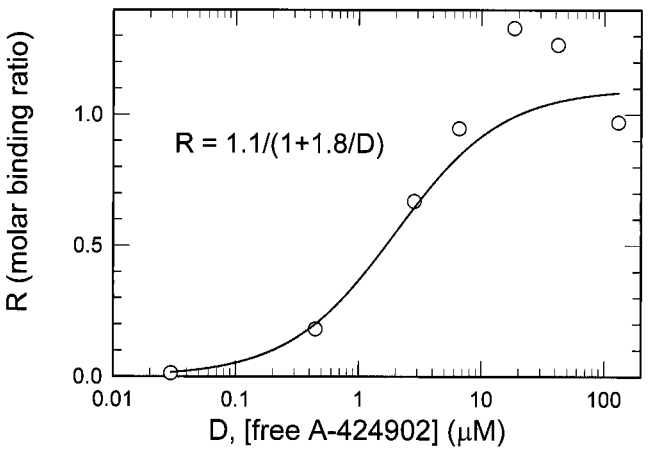

FIG. 5. Binding of [^{3}H]A-424902 to Phe-tRNA as determined by equilibrium dialysis. Binding mixtures contained 500 pmol of Phe-tRNA on one side of the membrane and known amounts of the drug on both sides. The radiolabeled drug concentration was kept constant at 100 nM, and the concentration of unlabeled A-424902 was varied. The binding isotherm was fitted by using the simple Hill equation shown.

tRNA truly reflects the binding mode in the tRNA-ribosome-mRNA complex. These questions, as well as the drug binding preference to $tRNA^{Phe}$, require further investigations.

We have also investigated the effect of A-424902 on the binding of radiolabeled $tRNA^{Phe}$ to 30S ribosomal subunits by using a nitrocellulose filter-binding technique (9) under the same reaction conditions for footprinting. The results showed that A-424902 did not affect quantitatively the binding of tRNA to 30S under these experimental conditions.

The present study demonstrates that members of the NRI series interact directly with tRNA and can alter the chemical footprint of tRNA on the ribosome. Although the footprinting behavior for the NRIs is similar to that of other 30S ribosome inhibitors, we note that no other drug classes behave in exactly the same way. These findings are consistent with the notion that the NRIs are mechanistically distinct. Based upon our findings, it seems reasonable to conclude that the NRIs affect the tRNA footprinting pattern at the decoding site on the 30S ribosomal subunit without affecting the overall binding free energy between tRNA and the ribosome.

REFERENCES

1. **Blaha, G., U. Stelzl, C. M. Spahn, R. K. Agrawal, J. Frank, and K. H. Nierhaus.** 2000. Preparation of functional ribosomal complexes and effect of buffer conditions on tRNA positions observed by cryoelectron microscopy. Methods Enzymol. **317:**292–309.
2. **Brodersen, D. E., W. M. Clemons, Jr., A. P. Carter, R. J. Morgan-Warren, B. T. Wimberly, and V. Ramakrishnan.** 2000. The structural basis for the action of the antibiotics tetracycline, pactamycin, and hygromycin B on the 30S ribosomal subunit. Cell **103:**1143–1154.
3. **Carter, A. P., W. M. Clemons, D. E. Brodersen, R. J. Morgan-Warren, B. T. Wimberly, and V. Ramakrishnan.** 2000. Functional insights from the structure of the 30S ribosomal subunit and its interactions with antibiotics. Nature **407:**340–348.
4. **Clark, R. F., S. Wang, Z. Ma, M. Weitzberg, C. Motter, M. Tufano, R. Wagner, Y. G. Gu, P. J. Dandliker, C. G. Lerner, L. E. Chovan, Y. Cai, C. L. Black-Schaefer, L. Lynch, D. Kalvin, A. M. Nilius, S. D. Pratt, N. Soni, T. Zhang, X. Zhang, and B. A. Beutel.** 2004. Novel inhibitors of bacterial protein synthesis: structure-activity relationships for 1,8-naphthyridine derivatives incorporating position 3 and 4 variants. Bioorg. Med. Chem. Lett. **14:**3299–3302.
5. **Dandliker, P. J., S. D. Pratt, A. M. Nilius, C. Black-Schaefer, X. Ruan, D. L. Towne, R. F. Clark, E. E. Englund, R. Wagner, M. Weitzberg, L. E. Chovan, R. K. Hickman, M. M. Daly, S. Kakavas, P. Zhong, Z. Cao, C. A. David, X. Xuei, C. G. Lerner, N. B. Soni, M. Bui, L. L. Shen, Y. Cai, P. J. Merta, A. Y. Saiki, and B. A. Beutel.** 2003. Novel antibacterial class. Antimicrob. Agents Chemother. **47:**3831–3839.
6. **Fourmy, D., M. I. Recht, S. C. Blanchard, and J. D. Puglisi.** 1996. Structure of the A site of *Escherichia coli* 16S rRNA complexed with an aminoglycoside antibiotic. Science **274:**1367–1371.
7. **Fourmy, D., M. I. Recht, and J. D. Puglisi.** 1998. Binding of neomycin-class aminoglycoside antibiotics to the A-site of 16 S rRNA. J. Mol. Biol. **277:**347–362.
8. **Klotz, I. M.** 1974. Protein interactions with small molecules. Acc. Chem. Res. **7:**162–168.
9. **Lodmell, J. S., W. E. Tapprich, and W. E. Hill.** 1993. Evidence for a conformational change in the exit site of the *Escherichia coli* ribosome upon tRNA binding. Biochemistry **32:**4067–4072.
10. **Mascaretti, O. A.** 2003. Bacteria versus antibacterial agents: an integrated approach. ASM Press, Washington, D.C.
11. **Matassova, N. B., M. V. Rodnina, R. Endermann, H. P. Kroll, U. Pleiss, H. Wild, and W. Wintermeyer.** 1999. Ribosomal RNA is the target for oxazolidinones, a novel class of translational inhibitors. RNA **5:**939–946.
12. **Miyaguchi, H., H. Narita, K. Sakamoto, and S. Yokoyama.** 1996. An antibiotic-binding motif of an RNA fragment derived from the A-site-related region of *Escherichia coli* 16S rRNA. Nucleic Acids Res. **24:**3700–3706.
13. **Moazed, D., and H. F. Noller.** 1987. Chloramphenicol, erythromycin, carbomycin and vernamycin B protect overlapping sites in the peptidyl transferase region of 23S ribosomal RNA. Biochimie **69:**879–884.
14. **Moazed, D., and H. F. Noller.** 1987. Interaction of antibiotics with functional sites in 16S ribosomal RNA. Nature **327:**389–394.
15. **Moazed, D., and H. F. Noller.** 1989. Interaction of tRNA with 23S rRNA in the ribosomal A, P, and E sites. Cell **57:**585–597.
16. **Moazed, D., and H. F. Noller.** 1986. Transfer RNA shields specific nucleotides in 16S ribosomal RNA from attack by chemical probes. Cell **47:**985–994.
17. **Moazed, D., S. Stern, and H. F. Noller.** 1986. Rapid chemical probing of conformation in 16S ribosomal RNA and 30 S ribosomal subunits using primer extension. J. Mol. Biol. **187:**399–416.
18. **Pioletti, M., F. Schlunzen, J. Harms, R. Zarivach, M. Gluhmann, H. Avila, A. Bashan, H. Bartels, T. Auerbach, C. Jacobi, T. Hartsch, A. Yonath, and F. Franceschi.** 2001. Crystal structures of complexes of the small ribosomal subunit with tetracycline, edeine, and IF3. EMBO J. **20:**1829–1839.
19. **Poulsen, S. M., C. Kofoed, and B. Vester.** 2000. Inhibition of the ribosomal peptidyl transferase reaction by the mycarose moiety of the antibiotics carbomycin, spiramycin, and tylosin. J. Mol. Biol. **304:**471–481.
20. **Pratt, S. D., C. A. David, C. Black-Schaefer, P. J. Dandliker, X. Xuei, U. Warrior, D. Burns, P. Zhong, Z. Cao, A. Y. C. Saiki, C. G. Lerner, L. E. Chovan, N. B. Soni, A. M. Nilius, F. L. Wagenaar, P. J. Merta, L. M. Traphagen, and B. A. Beutel.** 2004. A strategy for discovery of novel broad-spectrum antibacterials using a high-throughput *Streptococcus pneumoniae* transcription/translation screen. J. Biomol. Screening **9:**3–11.
21. **Purohit, P., and S. Stern.** 1994. Interactions of a small RNA with antibiotic and RNA ligands of the 30S subunit. Nature **370:**659–662.
22. **Rasmussen, B., H. F. Noller, G. Daubresse, B. Oliva, Z. Misulovin, D. M. Rothstein, G. A. Ellestad, Y. Gluzman, F. P. Tally, and I. Chopra.** 1991. Molecular basis of tetracycline action: identification of analogs whose primary target is not the bacterial ribosome. Antimicrob. Agents Chemother. **35:**2306–2311.
23. **Recht, M. I., S. Douthwaite, and J. D. Puglisi.** 1999. Basis for prokaryotic specificity of action of aminoglycoside antibiotics. EMBO J. **18:**3133–3138.
24. **Recht, M. I., D. Fourmy, S. C. Blanchard, K. D. Dahlquist, and J. D. Puglisi.** 1996. RNA sequence determinants for aminoglycoside binding to an A-site rRNA model oligonucleotide. J. Mol. Biol. **262:**421–436.
25. **Schlunzen, F., R. Zarivach, J. Harms, A. Bashan, A. Tocilj, R. Albrecht, A. Yonath, and F. Franceschi.** 2001. Structural basis for the interaction of antibiotics with the peptidyl transferase centre in eubacteria. Nature **413:**814–821.
26. **Shen, L. L., J. Baranowski, J. Fostel, D. A. Montgomery, and P. A. Lartey.** 1992. DNA topoisomerases from pathogenic fungi: targets for the discovery of antifungal drugs. Antimicrob. Agents Chemother. **36:**2778–2784.
27. **Shen, L. L., J. Baranowski, and A. G. Pernet.** 1989. Mechanism of inhibition of DNA gyrase by quinolone antibacterials: specificity and cooperativity of drug binding to DNA. Biochemistry **28:**3879–3885.
28. **Shen, L. L., W. E. Kohlbrenner, D. Weigl, and J. Baranowski.** 1989. Mechanism of quinolone inhibition of DNA gyrase. Appearance of unique norfloxacin binding sites in enzyme-DNA complexes. J. Biol. Chem. **264:**2973–2978.
29. **Shen, L. L., L. A. Mitscher, P. N. Sharma, T. J. O'Donnell, D. W. Chu, C. S. Cooper, T. Rosen, and A. G. Pernet.** 1989. Mechanism of inhibition of DNA gyrase by quinolone antibacterials: a cooperative drug-DNA binding model. Biochemistry **28:**3886–3894.
30. **Shen, L. L., and A. G. Pernet.** 1985. Mechanism of inhibition of DNA gyrase by analogues of nalidixic acid: the target of the drugs is DNA. Proc. Natl. Acad. Sci. USA **82:**307–311.
31. **Stern, S., D. Moazed, and H. F. Noller.** 1988. Structural analysis of RNA using chemical and enzymatic probing monitored by primer extension. Methods Enzymol. **164:**481–489.
32. **Sypherd, P. S., and J. W. Wireman.** 1974. Preparation of ribosomal subunits by large-scale zonal centrifugation. Methods Enzymol. **30:**349–354.
33. **Vicens, Q., and E. Westhof.** 2002. Crystal structure of a complex between the aminoglycoside tobramycin and an oligonucleotide containing the ribosomal decoding a site. Chem. Biol. **9:**747–755.
34. **Vicens, Q., and E. Westhof.** 2003. Crystal structure of Geneticin bound to a bacterial 16S ribosomal RNA A site oligonucleotide. J. Mol. Biol. **326:**1175–1188.
35. **Vicens, Q., and E. Westhof.** 2001. Crystal structure of paromomycin docked into the eubacterial ribosomal decoding A site. Structure **9:**647–658.
36. **Vicens, Q., and E. Westhof.** 2003. Molecular recognition of aminoglycoside antibiotics by ribosomal RNA and resistance enzymes: an analysis of x-ray crystal structures. Biopolymers **70:**42–57.
37. **Walsh, C.** 2003. Antibiotics: action, origins, resistance. ASM Press, Washington, D.C.